*Int. J. Multiphase Flow* Vol. 16, No. 3, pp. 461–479, 1990
Printed in Great Britain. 
0301-9322/90 $3.00 + 0.00


# AXIAL PRESSURE DISTRIBUTION IN TWO LATERALLY INTERCONNECTED CHANNELS WITH BLOCKAGES

A. TAPUCU,[1] A. TEYSSEDOU,[1] M. GEÇKINLI[2] and M. MERILO[3]
[1]Ecole Polytechnique, 2900 Edouard Montpetit, Montréal, Québec H3T 1J4, Canada
[2]Technical University of Istanbul, Ayazaga Kampusu, Maslak, Istanbul, Turkey
[3]Electric Power Research Institute, California, U.S.A.

(*Received* 3 *January* 1989; *in revised form* 5 *February* 1990)

**Abstract**—Pressure drop data obtained from two laterally interconnected channels, under two-phase (air–water) flow conditions is presented. Two types of blockages, plate and smooth, were used to restrict the flow area of one of the channels from 70 to 10% of its nominal value. The blockage induces large radial pressure differences between the channels, and the pressure equalization may require several hydraulic diameters before it is reached. The irreversible pressure loss produced by the blockage depends on the blockage shape and severity, and on the void distribution between the channels.

*Key Words:* two-phase, subchannels, blockages, pressure drop

## 1. INTRODUCTION

The consequence of a partial or complete blockage of a subchannel or a group of subchannels in a nuclear fuel bundle is to divert some, or all, of the flow into neighboring unblocked ones. Although the pressure equalization between the channels downstream of the blockage is a rapid process, the flow recovery within the blocked channel in the same region is, usually, a slow process. Several hydraulic diameters are required before the flow is restored to its far upstream value. Therefore, immediately downstream of the blockage, higher enthalpies will prevail in the blocked subchannels. The heat transfer in these regions may be impaired due to insufficient coolant, or enhanced because of increased turbulence. An adequate prediction of the enthalpies and heat transfer conditions in the downstream region requires detailed information on the flow redistribution caused by the blockage.

The aim of this paper is to present pressure drop data obtained from the two laterally interconnected channels when one of them is obstructed by blockages of various sizes. The data on void fraction and liquid and gas mass flow rates have been presented previously (Teyssedou *et al.* 1989a, b).

## 2. LITERATURE SURVEY

Data on the pressure distribution in interconnected subchannels with blockages and under two-phase flow conditions are, to the best of the author's knowledge, non-existent. However, some data have been obtained on the pressure field created by sudden area changes and by inserts in a single channel under single-phase flows by Lafay & Picut (1974), Sparrow *et al.* (1979) and Tapucu *et al.* (1984a), and for two-phase flows by Janssen & Kervinen (1964), Weisman *et al.* (1978), Salcudean *et al.* (1983a–c), Fairhurst (1983), Simpson *et al.* (1983), Chen *et al.* (1986) and Tapucu *et al.* (1988a). Aside from the axial pressure distribution, and in some cases radial pressure gradients (Lafay & Picut 1974; Sparrow *et al.* 1979), the investigators have mainly focused on the irreversible pressure losses caused by the flow area changes.

The experiments on two interconnected channels were motivated by the need for detailed information on the pressure field, and on the redistribution of the flow between the channels, when substantially different flow rates prevail at the beginning of the interconnected region. Data on pressures and liquid flow rates in interconnected channels without blockage have been presented by Tapucu & Merilo (1977a, b). One of the first two-channel experiments with a blockage in one of them was conducted with a single-phase fluid by Stiefel & Nothiger (1969; Stiefel 1971, 1972). They utilized two rectangular channels connected laterally by an adjustable gap formed by two oval

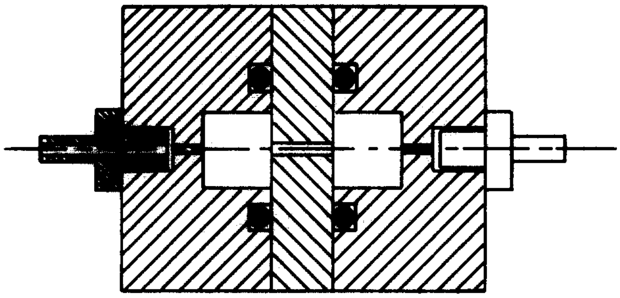

Figure 1. Cross-sectional view of the test section.

rods. A movable plate was used as a partial blockage. The authors observed that the upstream influence of the blockage on either the pressure or the mass flow rate could only be detected over a short distance (approx. 8 hydraulic diameters). Substantial pressure differences between the channels were observed in the region of high cross-flow velocities. Downstream of the blockage, the pressure equalization took place within a short distance (approx. 8 hydraulic diameters). However, a very gradual readjustment of the mass flow distribution was observed. Similar observations have also been made by Rowe (1973), Gençay *et al.* (1984) and Tapucu *et al.* (1984b).

The hydrodynamic behavior of two interconnected channels under two-phase flow conditions has been studied by Tapucu *et al.* (1982, 1988b). For unequal flow conditions at the beginning of the interconnected region, they produced detailed information on pressures, redistribution of void and liquid and gas mass flow rates between the channels.

## 3. EXPERIMENTAL APPARATUS

The details of the apparatus used to perform the blockage experiments have been given previously (1989a, b). The test section (figure 1) is made up of two 12.65 mm square channels machined from acrylic blocks. The channels are separated by an intermediate plate into which a long slot has been machined. The relevant geometric parameters of the test section are given in table 1. Plate and smooth blockages of varying size were mounted in channel 1 on the wall opposite the interconnection gap. The two-phase flow is generated by mixing the water and air in a mixer located upstream of the test section.

The pressure along the unblocked channel and pressure differences between the blocked and unblocked channels are measured with Statham pressure transducers every 38.1 mm. Far from the blockage, the measurement interval has been increased to 76.2 mm. The region over which the pressures were measured extends to 514 mm upstream and 857 mm downstream of the blockage. Figure 2 shows the locations at which the pressures were measured. After conditioning, the electrical signals from the pressure transducers were sent to an integrating digital voltmeter. This allowed measurement of the pressure over a predetermined time interval (usually 50 s) and determination of its mean value. According to manufacturer specifications, the combined

Table 1. Geometric parameters of the test section

| | |
|---|---|
| Gap clearance | 1.5 mm |
| Gap thickness | 3.2 mm |
| Hydraulic diameters | |
| Channel 1[a] | 12.7 mm |
| Channel 1 | 12.4 mm |
| Channel 2[a] | 12.8 mm |
| Channel 2 | 12.6 mm |
| Cross-sectional area | |
| Channel 1 | 160 $mm^2$ |
| Channel 1[a] | 162.4 $mm^2$ |
| Channel 2 | 163.1 $mm^2$ |
| Channel 2[a] | 165.5 $mm^2$ |
| Length of the interconnection | 1312 mm |

[a]Including half of the interconnecting gap. The mid-plane of the blockage is located 272 mm downstream of the interconnection.

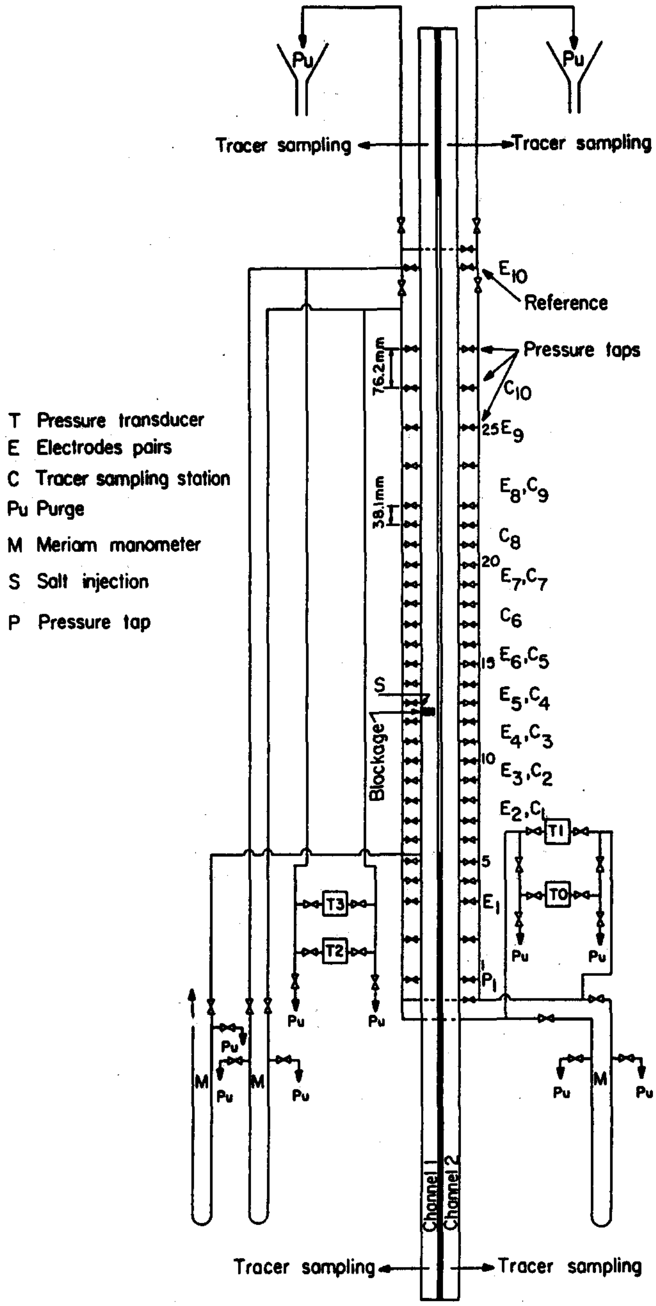


Figure 2. Location of pressure taps, void gauges and tracer sampling stations.

nonlinearity and hysteresis errors of the pressure transducers are $<1\%$. The pressure in the blocked channel, 272 mm upstream of the blockage, is measured relative to the atmospheric pressure with a Meriam manometer. Therefore, the absolute pressure along the channel can be determined.

Two blockage configurations were studied: plate and smooth. The shape of the latter was a cosine defined as

$$y = H \cos\left(\frac{\pi z}{L}\right), \qquad [1]$$

where $H$ is the blockage height, $z$ is the axial length and $L$ is the blockage length.

The plate blockage could be moved continuously in the radial direction to adjust the blockage area. Table 2 gives the geometric parameters of the blockages.

Table 2

| | | | |
|---|---|---|---|
| *Plate Blockage* | | | |
| Area reduction (%)[a] | 31.9 | 61.0 | 90.0 |
| Thickness, $L$ (mm) | 3.2 | 3.2 | 3.2 |
| Height, $H$ (mm) | 4.1 | 7.9 | 11.6 |
| *Smooth Blockage* | | | |
| Area reduction (%)[a] | 58.0 | | 88.12 |
| Length, $L$ (mm) | 49.9 | | 50.5 |
| Height, $H$ (mm) | 7.5 | | 11.4 |

[a]Including half of the interconnecting gap.

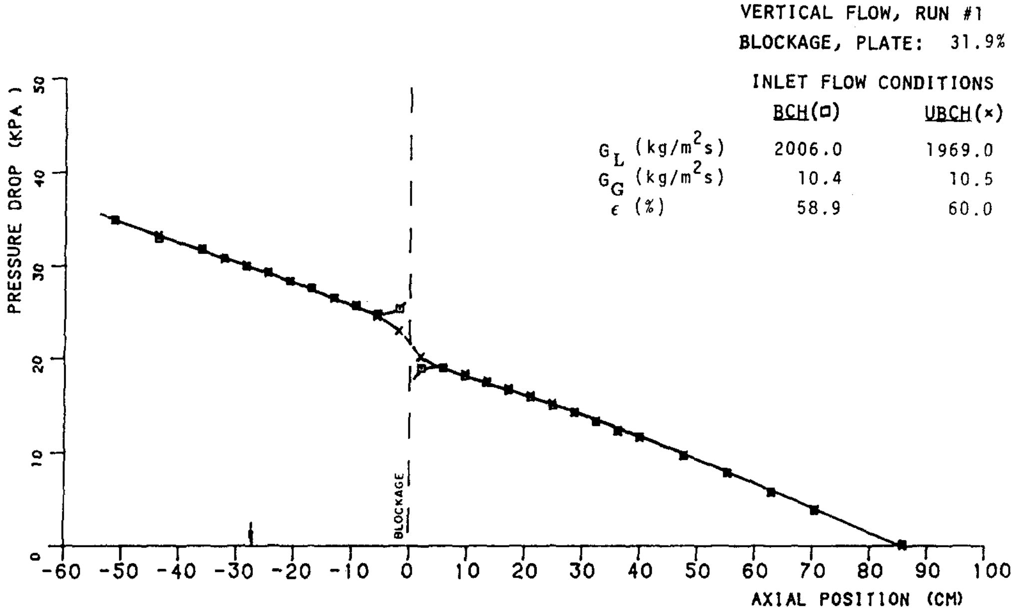


Figure 3a. Pressures in the blocked (BCH) and unblocked (UBCH) channels.

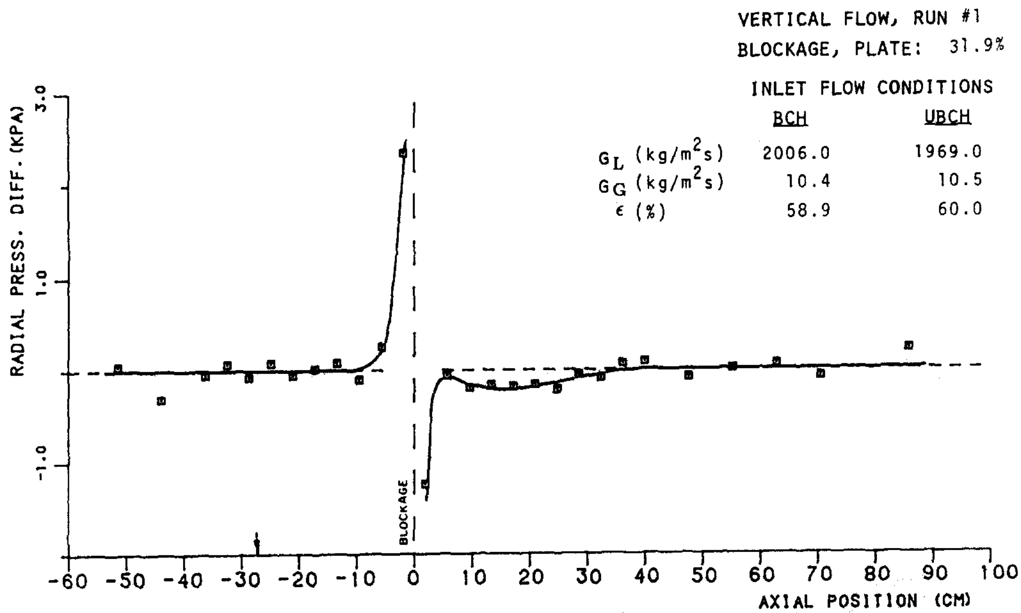


Figure 3b. Pressure differences between the blocked (BCH) and unblocked (UBCH) channels.

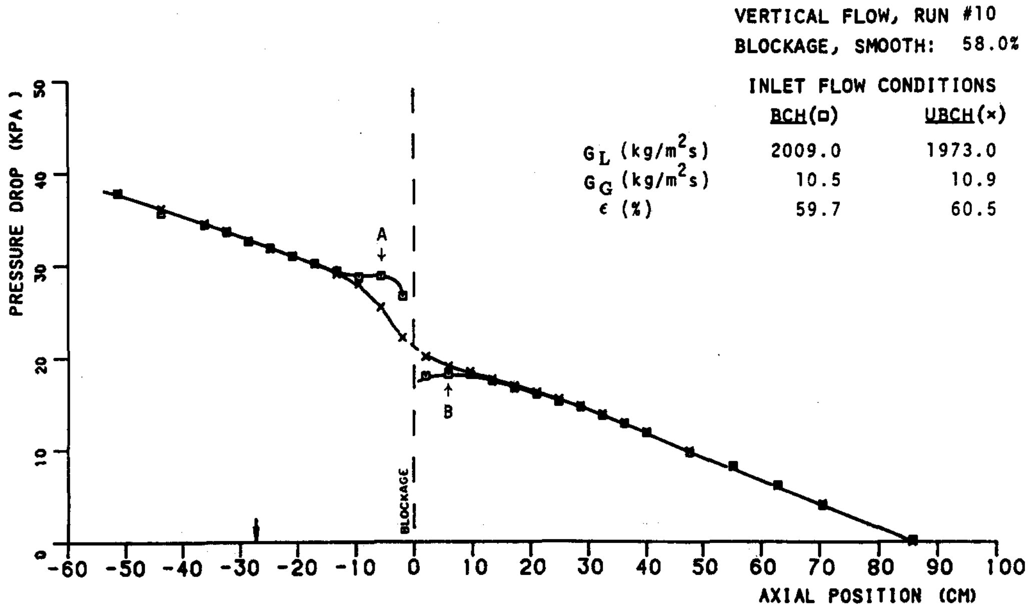


Figure 4a. Pressures in the blocked (BCH) and unblocked (UBCH) channels.

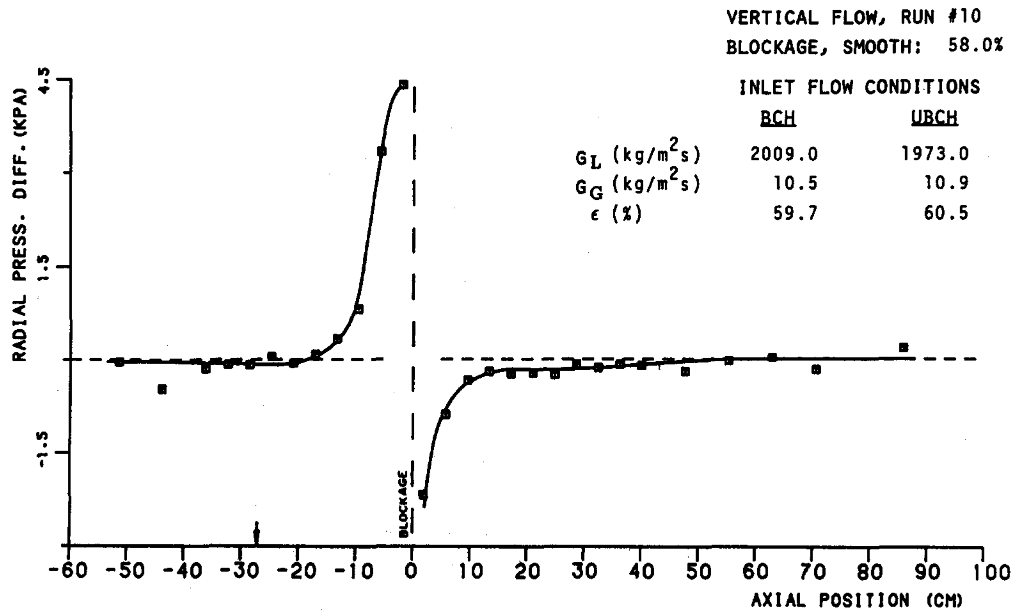


Figure 4b. Pressure differences between the blocked (BCH) and unblocked (UBCH) channels.

## 4. EXPERIMENTAL RESULTS

Three blockage fractions have been used for plate blockages (30, 60 and 90%), whereas smooth blockages were limited to blockage fractions of 60 and 90%. For each blockage fraction a set of three experiments were generally conducted:

1. Equal inlet void fractions: 60% at the inlet of each channel.
2. Unequal inlet void fractions with high void at the inlet of the blocked channel: 60 and 0% void fractions at the inlet of the blocked and unblocked channels, respectively.
3. Unequal inlet void fractions with high void at the inlet of the unblocked channel: 0 and 60% void fractions at the inlet of the blocked and unblocked channels, respectively.

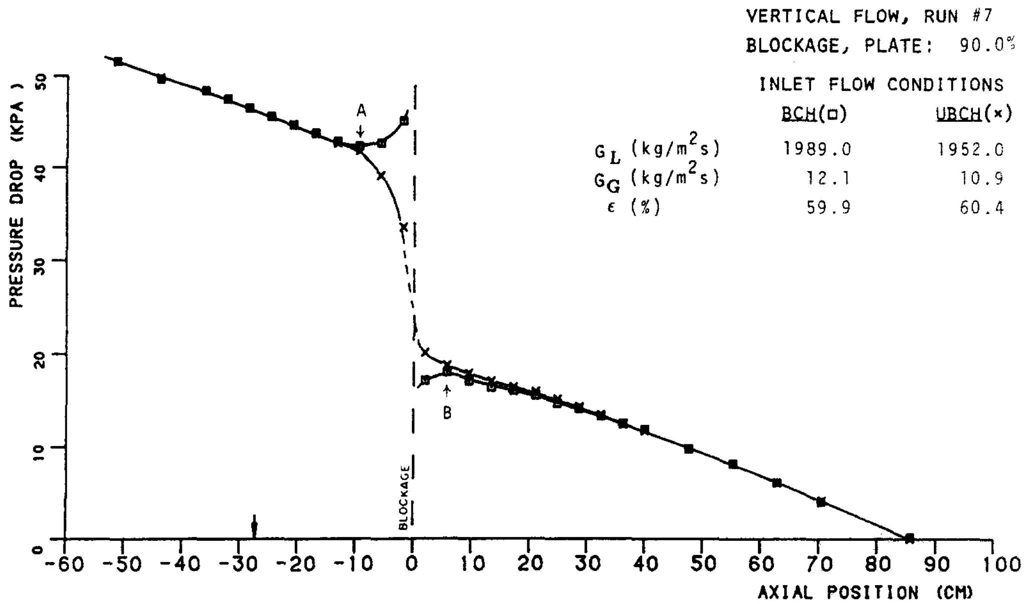


Figure 5a. Pressures in the blocked (BCH) and unblocked (UBCH) channels.

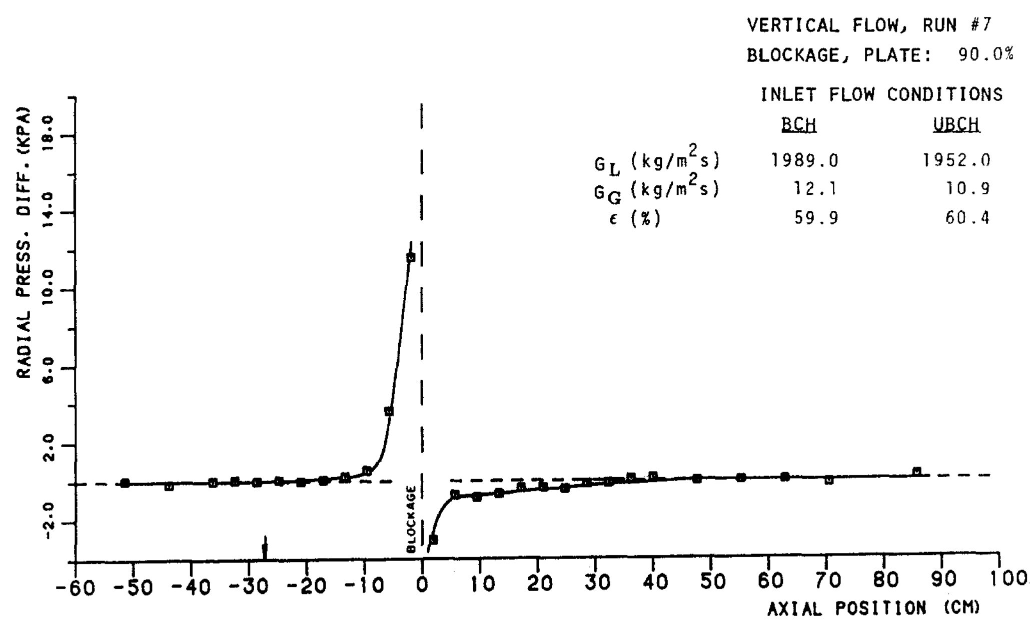


Figure 5b. Pressure differences between the blocked (BCH) and unblocked (UBCH) channels.

Only the pressure field obtained for 30 and 90% plate blockages, and for a 60% smooth blockage are presented in this paper. More data on pressures are given in Tapucu *et al.* (1988a).

## *Axial Pressures*

### *Equal void fractions at the inlet of the blocked and unblocked channels*

The pressures upstream of the blockage in the blocked and unblocked channels are equal and decrease quite linearly up to the point of onset of diversion cross-flow caused by the blockage (figures 3a–5a). For plate blockages, starting from this point, the pressure increases in the blocked channel and decreases in the unblocked channel (figures 3a and 5a). The increase in pressure in the blocked channel is due to the fact that the pressure gains, caused by the stagnation of the flow by the blockage and the deceleration resulting from the mass transfer to the unblocked channel, is far greater than the pressure loss due to the wall friction (in the channel and interconnected region). The situation for smooth blockages is somewhat different: starting from the point of onset of diversion cross-flow (figure 4a), the pressure in the blocked channel first increases slightly, showing that the pressure rise is slightly higher than pressure loss, and then decreases. This decrease is caused by the acceleration of the flow within the blocked region up to the vena contracta. In turn, the pressures in the unblocked channel, for both type of blockages, decrease regularly due to the acceleration caused by the lateral inflow.

In the blocked channel, the substantial pressure drop within the blocked zone is mainly the consequence of the flow acceleration up to the vena contracta and the energy dissipation due to vortex formation. Downstream of the blockage, only partial pressure recovery occurs and is due simultaneously to the deceleration of the flow during the expansion from the vena contracta to the flow section of the channel, and to the deceleration of the lateral inflow. As long as the gains in pressure are higher than the losses, the pressure in the blocked channel increases. When the equilibrium between the gains and losses is established, the pressure goes through a maximum and then starts decreasing. The pressure recovery in the blocked channel is accomplished over a distance of 60 mm (5 hydraulic diameters) downstream of the blockage, irrespective of the blockage shape and severity and the void fraction. In the unblocked channel, mainly because of the deceleration of the flow, the pressure drops gradually until it equals the pressure variation in the blocked channel.

The difference between the minimum pressure in the blocked channel upstream of the blockage and the maximum pressure downstream of the blockage (points **A** and **B**, respectively, in figure 5a) accounts for the irreversible pressure drop caused by the blockage, and the friction and acceleration pressure drop as well. As pointed out by Tapucu *et al.* (1988a), the irreversible pressure loss caused by the blockage depends on the blockage severity, on the blockage shape and on the void fraction.

Between the beginning of the interconnected region and the point of onset of diversion cross-flow (Teyssedou *et al.* 1989b), the pressure gradients in both channels are almost constant. However, some variation in the pressure gradient is observed in the downstream region of the blockage. This variation is mainly due to the mass exchange between the channels and to the expansion of the gas due to decreasing pressure. It is only very far from the blockage that the pressure gradient can be considered as constant.

*Unequal void fractions at the inlet of the blocked and unblocked channels*

The pressure gradients, which were substantially different before the interconnection, assume equal values almost at the beginning of the interconnection (figures 6a–11a). The behavior of the pressure in the interconnected region upstream and downstream of the blockage is very similar to that observed for equal void fractions at the inlet of the channels.

### *Pressure Difference Between the Channels*

*Equal void fractions at the inlet of blocked and unblocked channels*

For symmetrical flow conditions at the inlet of the blocked and unblocked channels, no pressure difference is observed between the channels upstream and immediately downstream of the beginning of the interconnected region (figures 3a–5a). The effect of the blockage is felt first as a gradual and then as a rapid increase in the pressure difference between the channels, which drives some of the flow from the blocked to the unblocked channel. For the 30% plate blockage, the effect of the obstruction on the pressure differences is felt approx. 100 mm (8 hydraulic diameters) upstream of the blockage (figure 3b), while for the 60% smooth and 90% plate blockages this effect is felt approx. 170 mm (14 hydraulic diameters) upstream of the blockage (figures 4b and 5b).

Downstream of the obstruction, because of the acceleration of the flow up to the vena contracta and the dissipation of mechanical energy in the wake zone, the pressure in the blocked channel drops faster than that in the unblocked channel and causes a fast pressure tilt in favor of the unblocked channel. With this tilt, the pressure is now higher in the unblocked channel and drives the previously diverted flow back to the blocked channel. The recovery in the blocked channel of the reversible portion of the pressure drop on one hand, and the kinetic energy of the lateral inflow on the other hand, rapidly reduces the pressure difference between the channels. However, the

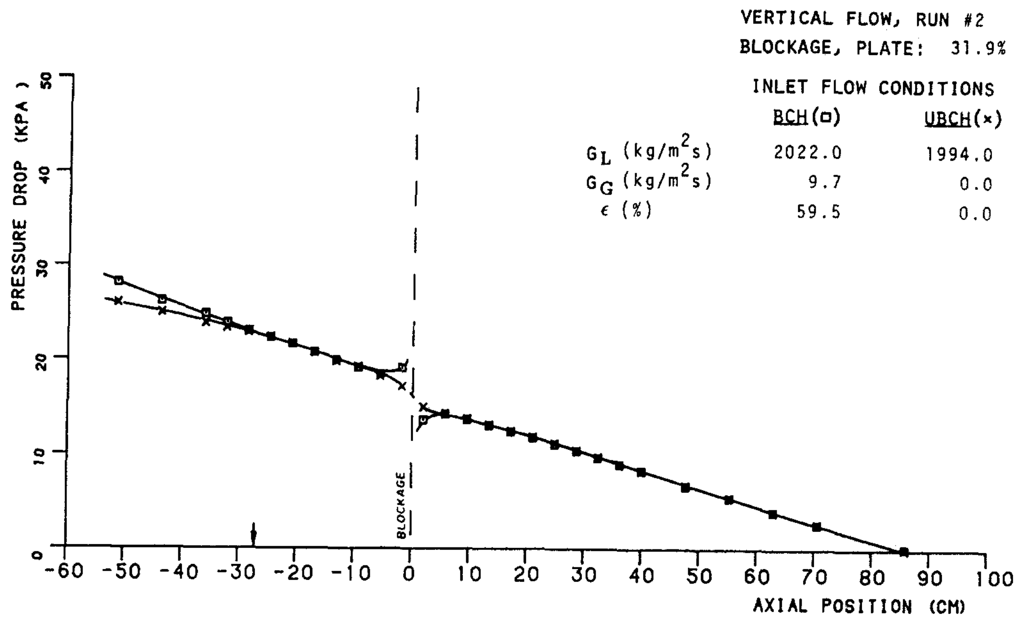


Figure 6a. Pressures in the blocked (BCH) and unblocked (UBCH) channels.

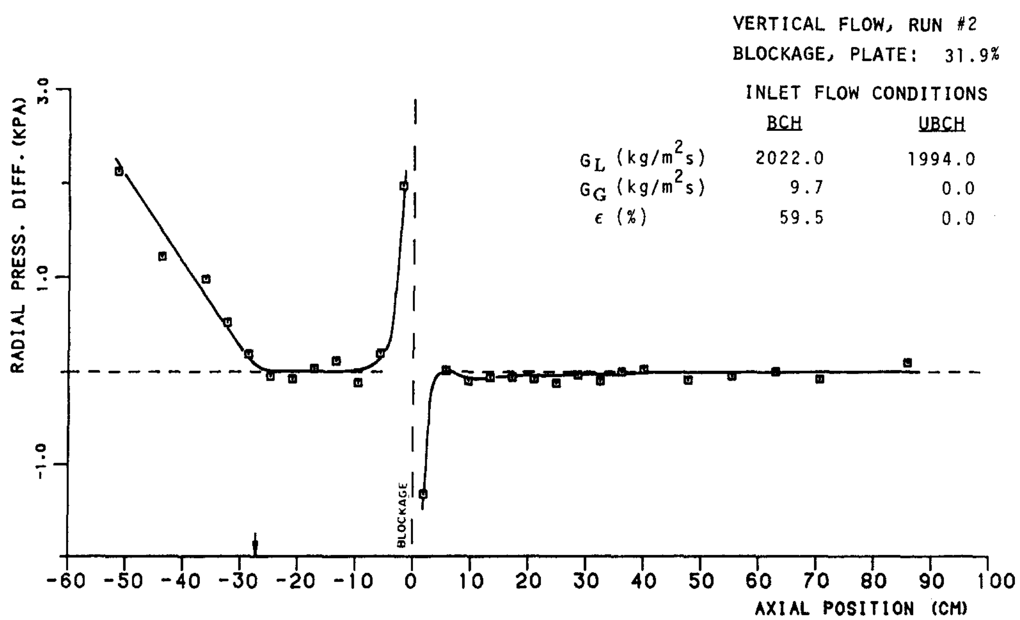


Figure 6b. Pressure differences between the blocked (BCH) and unblocked (UBCH) channels.

complete equalization of the pressures in the channels requires a distance of approx. 360 mm (30 hydraulic diameters) under the present experimental conditions. Therefore, in contrast to single-phase flow (Tapucu *et al.* 1984b), the pressure equalization between the two channels is not a rapid process.

*Unequal void fractions at the inlet of the blocked and unblocked channels*

The substantial pressure difference observed upstream of the interconnected region is the consequence of the different inlet flow conditions to the channels (figures 6b–11b). This difference decreases rapidly as the flow approaches the beginning of the interconnected region. The pressure equalization is achieved mainly by the transfer of liquid from the high pressure channel to the low pressure channel, until the effect of the blockage is felt on the flow.

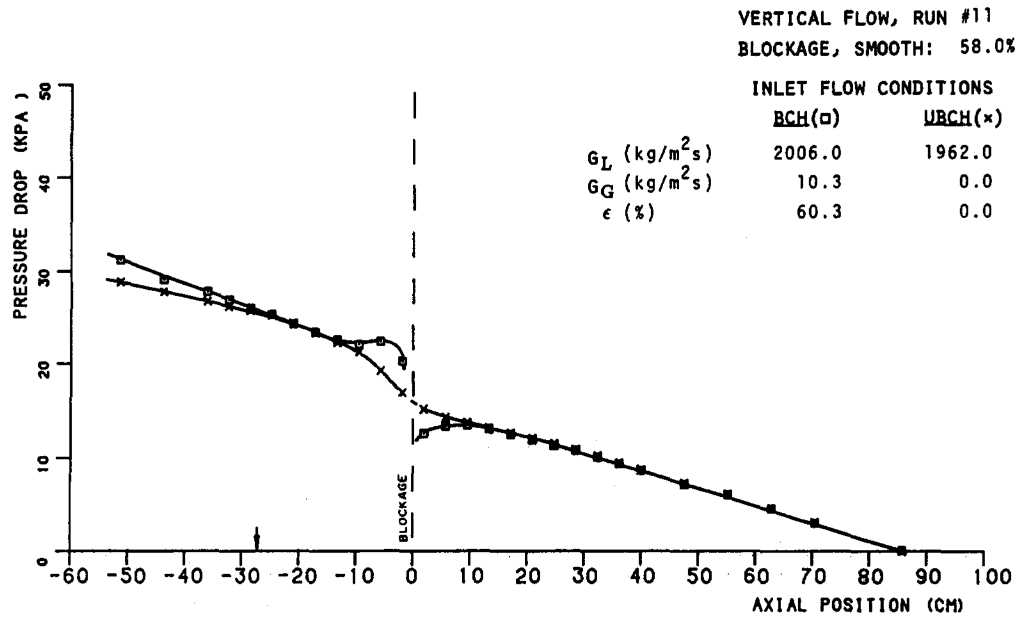


Figure 7a. Pressures in the blocked (BCH) and unblocked (UBCH) channels.

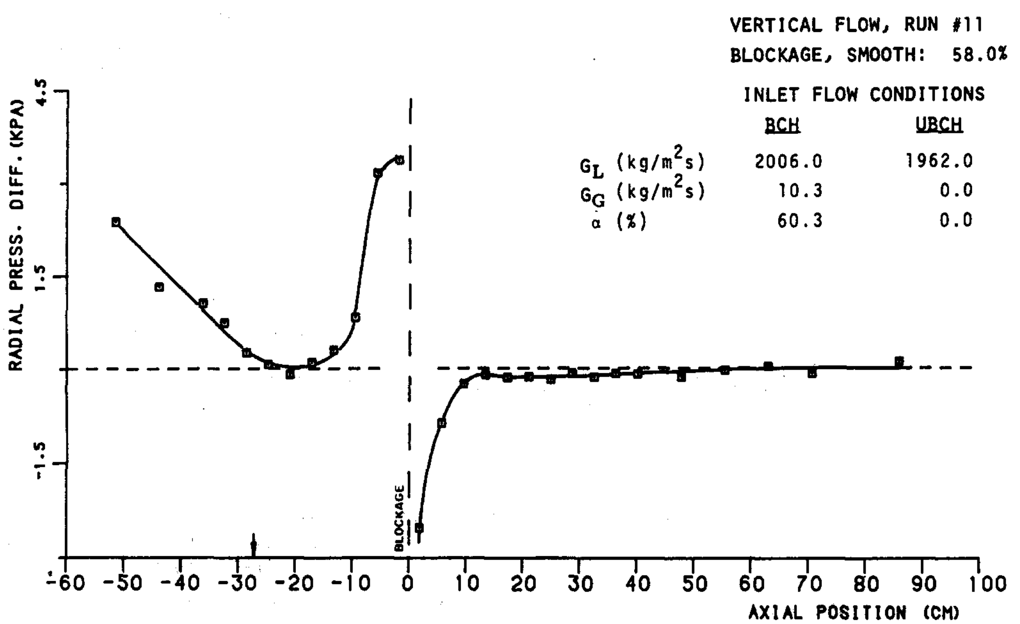


Figure 7b. Pressure differences between the blocked (BCH) and unblocked (UBCH) channels.

The behavior of the pressure differences in the upstream region close to the blockage is similar to that of identical flow conditions at the inlet of the channels, i.e. a rapid increase in the pressure in the blocked channel which drives some of the flow to the unblocked channel. The effect of the blockage on the pressure differences is again felt approx. 100 mm in the upstream region for 30% plate blockage and 170 mm for 60% smooth and 90% plate blockages. For plate blockages, the pressure difference increases until the last measurement point upstream from the blockage. However, the 60% smooth blockage showed a decrease (figure 10b) or a tendency for decrease (figures 4b and 7b) at this measurement point which is in the blocked region. This decrease is very likely due to the acceleration of the flow to the vena contracta which may form just upstream of the mid-plane of the blockage.

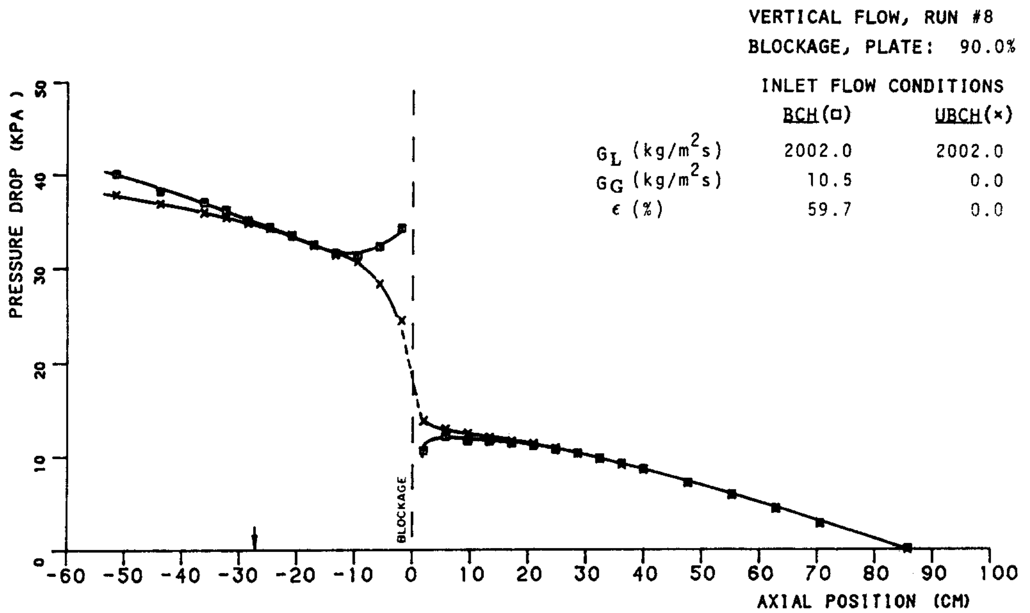


Figure 8a. Pressures in the blocked (BCH) and unblocked (UBCH) channels.

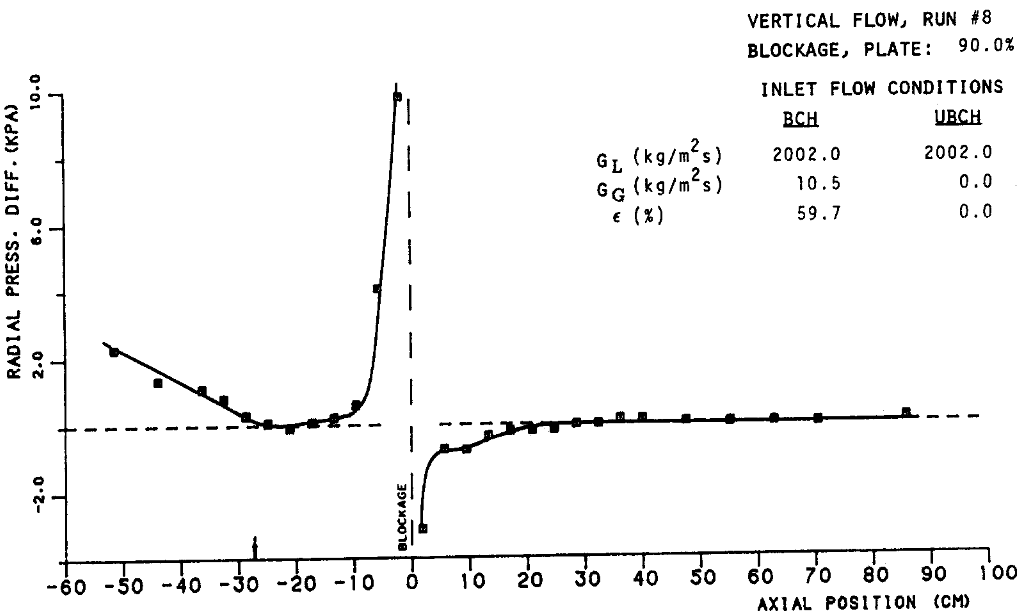


Figure 8b. Pressure differences between the blocked (BCH) and unblocked (UBCH) channels.

In the downstream region, the pressure equalization between the channels occurs between 300 and 500 mm (25 and 40 hydraulic diameters) depending on the blockage shape and severity, and the inlet flow conditions to the channels.

## 5. IRREVERSIBLE PRESSURE LOSSES CAUSED BY BLOCKAGES IN INTERCONNECTED CHANNELS

Using an approach similar to that given in Tapucu *et al.* (1988a), the irreversible pressure losses caused by the blockage can be written as

$$\Delta p_b = \Delta p_{\text{form}} + \Delta p_{\text{friction}} + \Delta p_{\text{gravity}}. \qquad [2]$$

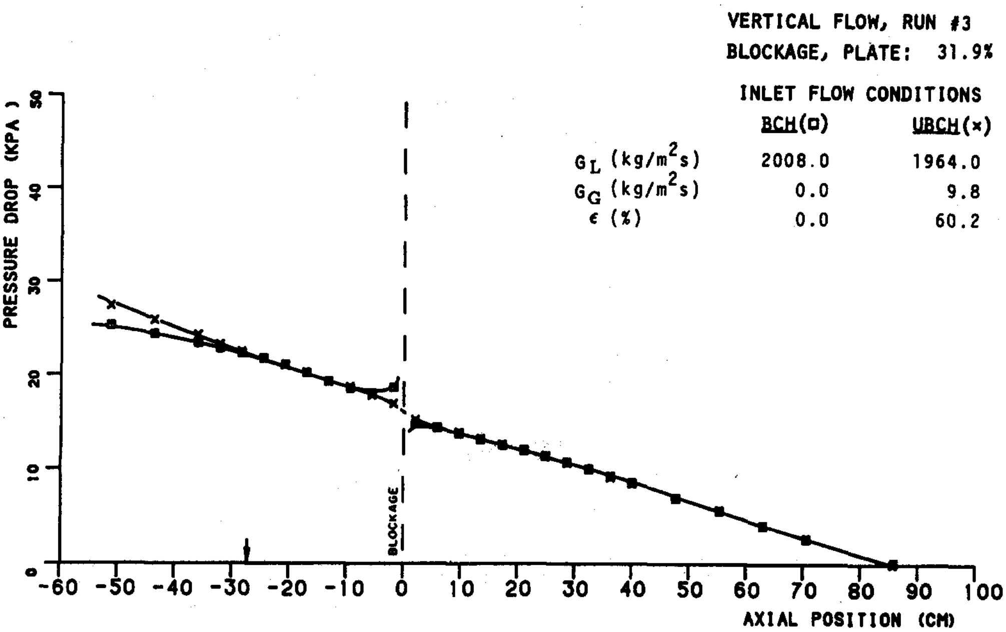


Figure 9a. Pressures in the blocked (BCH) and unblocked (UBCH) channels.

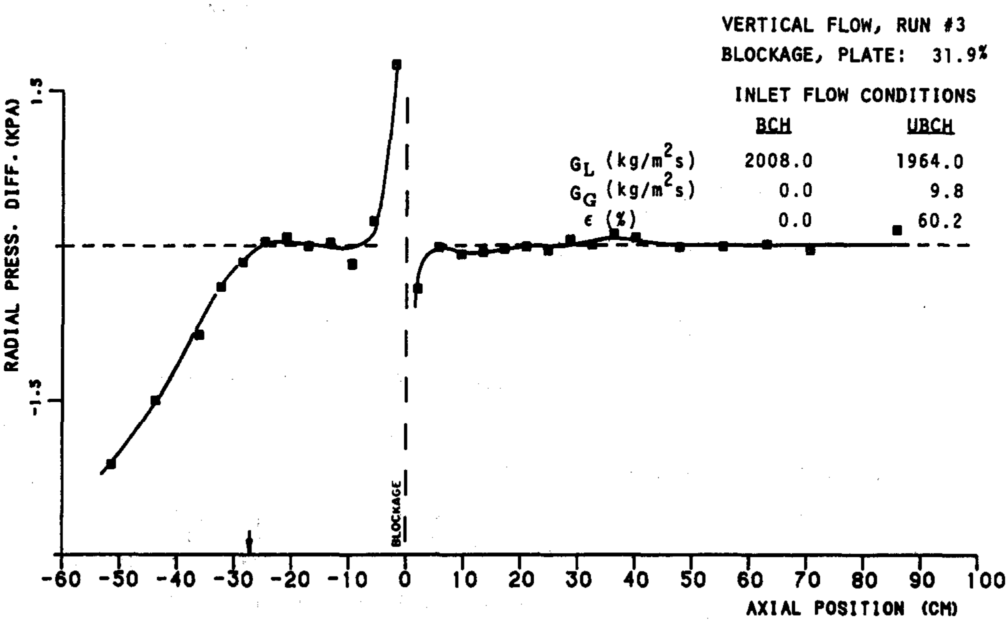


Figure 9b. Pressure differences between the blocked (BCH) and unblocked (UBCH) channels.

$\Delta p_{\text{form}}$ is mainly due to the dissipation of the mechanical energy as heat in the recirculation zone which forms behind the blockage. As pointed out in Tapucu *et al.* (1988a), this term also contains the acceleration pressure drop due to the expansion of the gas with the sudden decrease of pressure in the blocked region. Since the importance of the recirculation zone depends on the severity and shape of the blockage, it is probable that these two parameters play an important role in the form pressure drop.

The form pressure drop will be modeled by introducing an irreversible pressure loss coefficient $K$:

$$\Delta p_{\text{form, TP}} = -K\frac{G^2}{2\rho'}, \qquad [3]$$

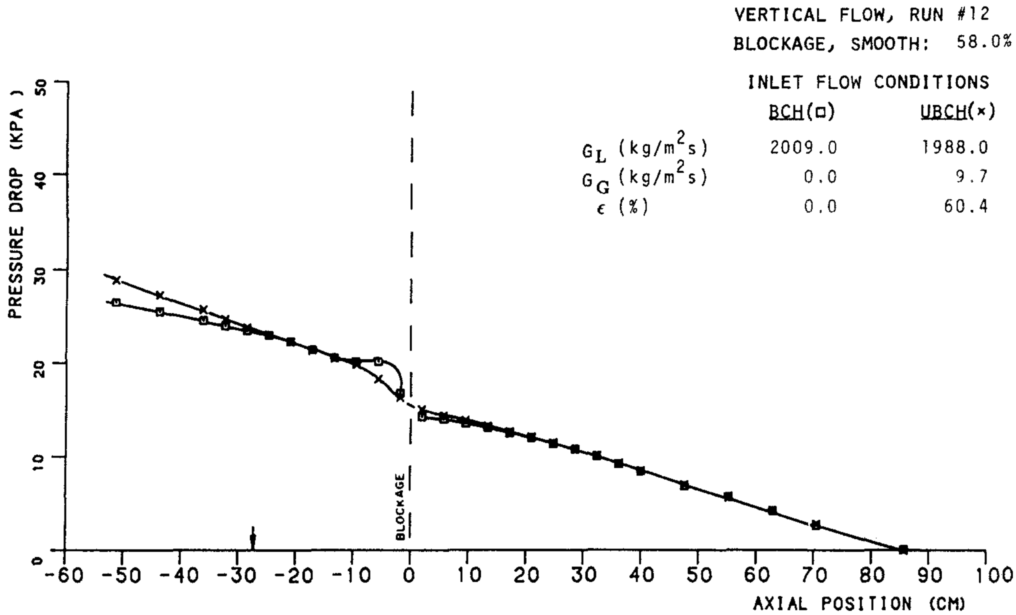


Figure 10a. Pressures in the blocked (BCH) and unblocked (UBCH) channels.

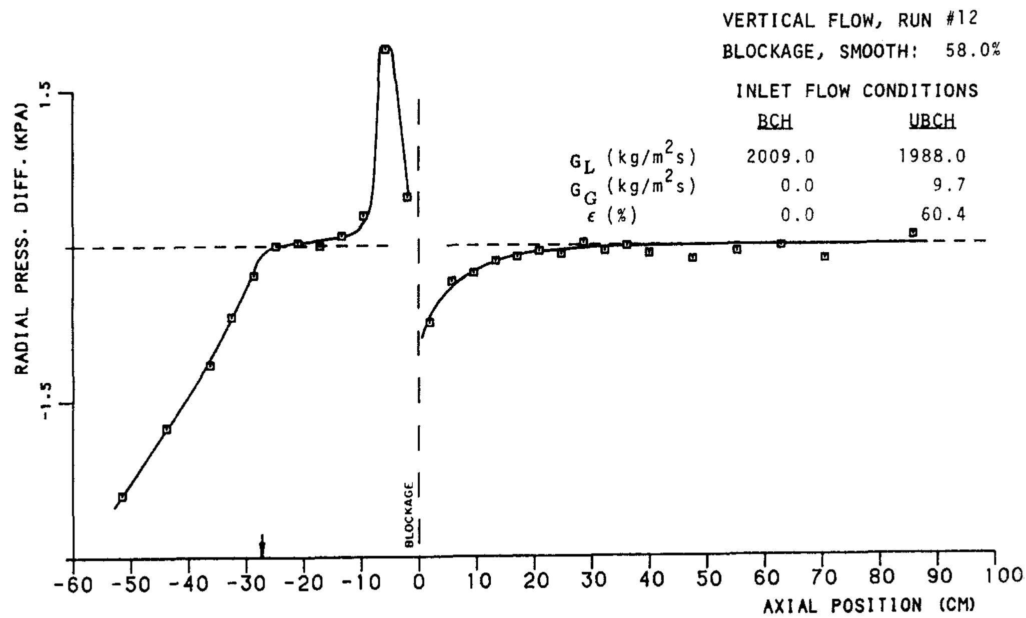


Figure 10b. Pressure differences between the blocked (BCH) and unblocked (UBCH) channels.

where $G$ is the mass flux and $\rho'$ is the momentum density. In turn, the two-phase multiplier is defined by

$$\Phi^2_{\text{form}} = \frac{\Delta p_{\text{form, TP}}}{\Delta p_{\text{form, SP}}} = \frac{K_{\text{TP}}}{K_{\text{SP}}} \frac{\rho_{\text{L}}}{\rho'}, \qquad [4]$$

where $\Delta p_{\text{form, SP}}$ is the form pressure loss when all the mixture flows as liquid in the channels. $\Delta p_{\text{form, SP}}$ is determined using the data given in Tapucu *et al.* (1984a).

For plate blockages in a single channel the irreversible pressure loss, $\Delta p_{\text{b}}$, is customarily determined by extrapolating the linear pressure variation upstream and downstream of the blockage to the mid-plane of the blockage (Lafay & Picut 1974; Sparrow *et al.* 1979; Tapucu *et al.* 1984a, 1989). For smooth blockages, Tapucu *et al.* (1984a, 1989) determined the irreversible pressure loss by extrapolating the linear pressure variations to the lower and upper planes which

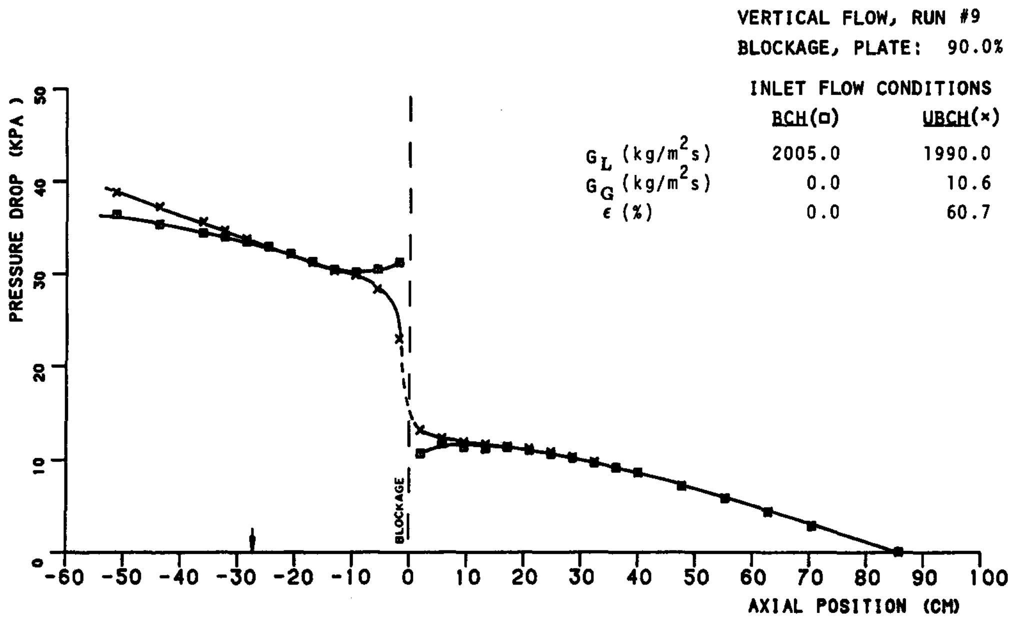


Figure 11a. Pressures in the blocked (BCH) and unblocked (UBCH) channels.

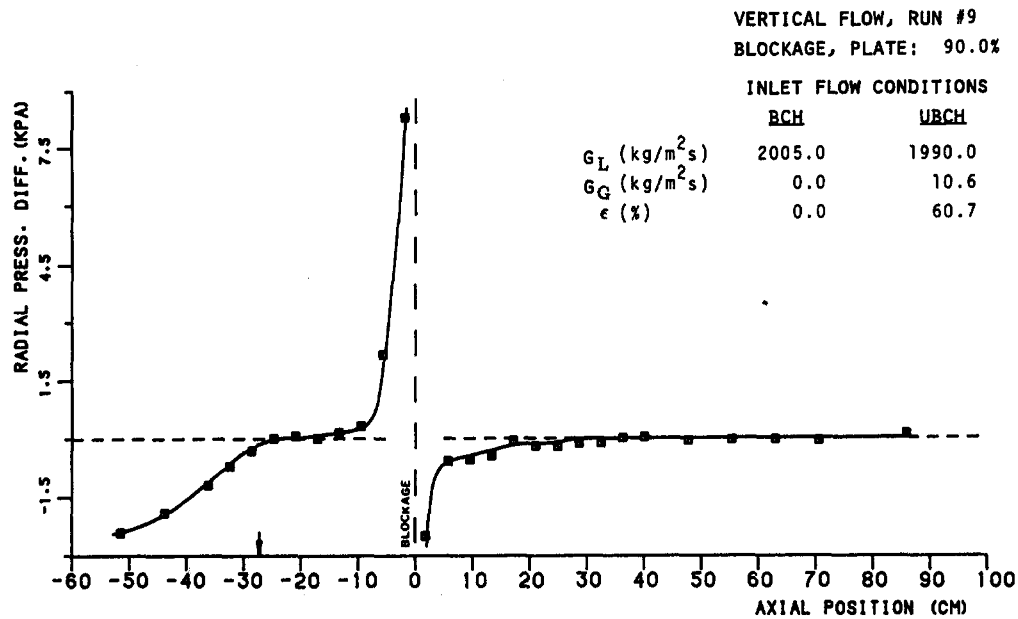


Figure 11b. Pressure differences between the blocked (BCH) and unblocked (UBCH) channels.

limit the blockage. However, under two-channel flow conditions, due to the transverse inflows and outflows, the variation of the axial pressures upstream and downstream of the blockage is not linear, which renders the application of the above procedure difficult. To circumvent this difficulty, the pressure difference in the blocked channel between the minimum pressure upstream of the blockage and the maximum pressure in the downstream region (points **A** and **B** in figures 4a and 5a) is considered and the form pressure drop is then obtained by subtracting the friction and gravity pressure loss components from this difference:

$$\Delta p_{\text{form}} = (p_B - p_A) + \Delta p_{\text{friction}} + \Delta p_{\text{gravity}}. \qquad [5]$$

The overall blockage fraction is determined by using the combined flow section of the channels including the interconnection. Since the flow areas of the channels are equal and that corresponding to the interconnection is small, the blockage fraction by this definition is, for all practical purposes, one-half of that based on the flow area of one channel.

*Plate Blockage*

For plate blockages, the friction and gravity losses appearing in [5] are deduced from the linear pressure variation far downstream of the blockage, where mass exchanges between the channels are small and equilibrium conditions have almost been reached. The slope of this variation, $(\mathrm{d}p/\mathrm{d}z)_{TP}$, determined by linear regression on the experimental points, contains the three components of the pressure drop: friction, acceleration and gravity. The acceleration term is usually small compared to the other components. The irreversible form pressure loss of the blockage is then given by

$$\Delta p_{\mathrm{form,TP}} = (p_{\mathrm{B}} - p_{\mathrm{A}}) - \left(\frac{\mathrm{d}p}{\mathrm{d}z}\right)_{\mathrm{TP}} \Delta z, \quad [6]$$

where $\Delta z$ is the distance between the minimum pressure upstream and the maximum pressure downstream of the blockage (points **A** and **B** in figures 4a and 5a).

The irreversible form pressure loss coefficient and the form two-phase multiplier have been calculated using [3] and [4]. The momentum density, $\rho'$, appearing in [3] is determined by using the flow dryness fraction at the inlet of the test section:

$$x = \frac{W_{\mathrm{G1}} + W_{\mathrm{G2}}}{W_1 + W_2}, \quad [7]$$

where $W$ is the mass flow rate.

The void fraction corresponding to the above dryness fraction is determined by using the flow dryness fraction–void fraction relationship obtained experimentally under single-channel flow conditions (Tapucu *et al.* 1988a). In turn, the absolute pressure at the mid-plane of the blockage is used to determine the density of the gas.

Table 3 gives the irreversible form pressure loss coefficients and two-phase multipliers obtained under two-channel flow conditions. The variation of the pressure loss coefficient with blockage fraction is illustrated in figure 12. This figure also includes the irreversible form pressure drop coefficients obtained under single-channel flow conditions for a 60% void fraction (Tapucu *et al.* 1989) and the experimental data obtained by Stiefel (1971), Rowe *et al.* (1973), Fairhurst (1983) and Tapucu *et al.* (1984a). It is observed that the irreversible form pressure loss coefficient for plate blockages is quite independent of the void fraction determined with the above procedure and its value is higher than that of an equivalent blockage in a single channel. These higher values can be attributed to the irreversible pressure losses occurring in the interconnection gap due to the substantial diversion cross-flow induced by the blockage. These losses originate from the friction in the gap region and from the contraction of the transverse flow followed by an expansion.

From table 3 it is observed that the irreversible form pressure loss coefficient depends on the void distribution between the channels and smaller values of this coefficient result when a high void is introduced in the unblocked channel.

Table 3. Irreversible form pressure loss coefficient for two interconnected channels (plate blockages)

| Run No. | Blockage fraction (%) | Dryness fraction $\bar{x}$ | Void fraction $\bar{\epsilon}$ | $\rho'$ (kg/m$^3$) | Absolute pressure (kPa) | $(\Delta p_{\mathrm{AB}})_{\mathrm{TP}}$ (Pa) | $\Delta p_f + \Delta p_g$ (Pa) | $\Delta p_{\mathrm{form,TP}}$ (Pa) | $\Delta p_{\mathrm{form,SP}}$ (Pa)[a] | $K_{\mathrm{form,TP}}$ | $\Phi^2_{\mathrm{form}}$ |
|---|---|---|---|---|---|---|---|---|---|---|---|
| 1 | 31.9 | 0.00523 | 0.61 | 391.2 | 151.16 | −5809.1 | −1871.6 | −3937.5 | −650.0 | 0.78 | 6.06 |
| 2 | 31.9 | 0.00240 | 0.48 | 517.6 | 137.59 | −4169.3 | −2057.9 | −2111.4 | −650.0 | 0.54 | 3.25 |
| 3 | 31.9 | 0.00248 | 0.48 | 513.2 | 137.64 | −3252.0 | −1404.9 | −1847.1 | −650.0 | 0.48 | 2.84 |
| 4 | 61.0 | 0.00564 | 0.61 | 385.2 | 155.94 | −11533.5 | −3038.0 | −8495.5 | −2125.0 | 1.64 | 4.00 |
| 5 | 61.0 | 0.00252 | 0.49 | 511.6 | 142.00 | −8566.7 | −2109.1 | −6457.6 | −2125.0 | 1.67 | 3.04 |
| 6 | 61.0 | 0.00232 | 0.48 | 521.3 | 138.08 | −8225.4 | −2081.5 | −6143.9 | −2125.0 | 1.63 | 2.89 |
| 7 | 90.0 | 0.00579 | 0.62 | 383.5 | 160.73 | −24348.7 | −3838.5 | −20510.2 | −5805.0 | 4.05 | 3.53 |
| 8 | 90.0 | 0.00260 | 0.49 | 507.3 | 144.29 | −19192.8 | −2800.6 | −16392.2 | −5805.0 | 4.15 | 2.82 |
| 9 | 90.0 | 0.00268 | 0.50 | 503.5 | 143.31 | −18420.9 | −2804.6 | −15616.4 | −5805.0 | 3.94 | 2.69 |

[a]Tapucu *et al.* (1984a).

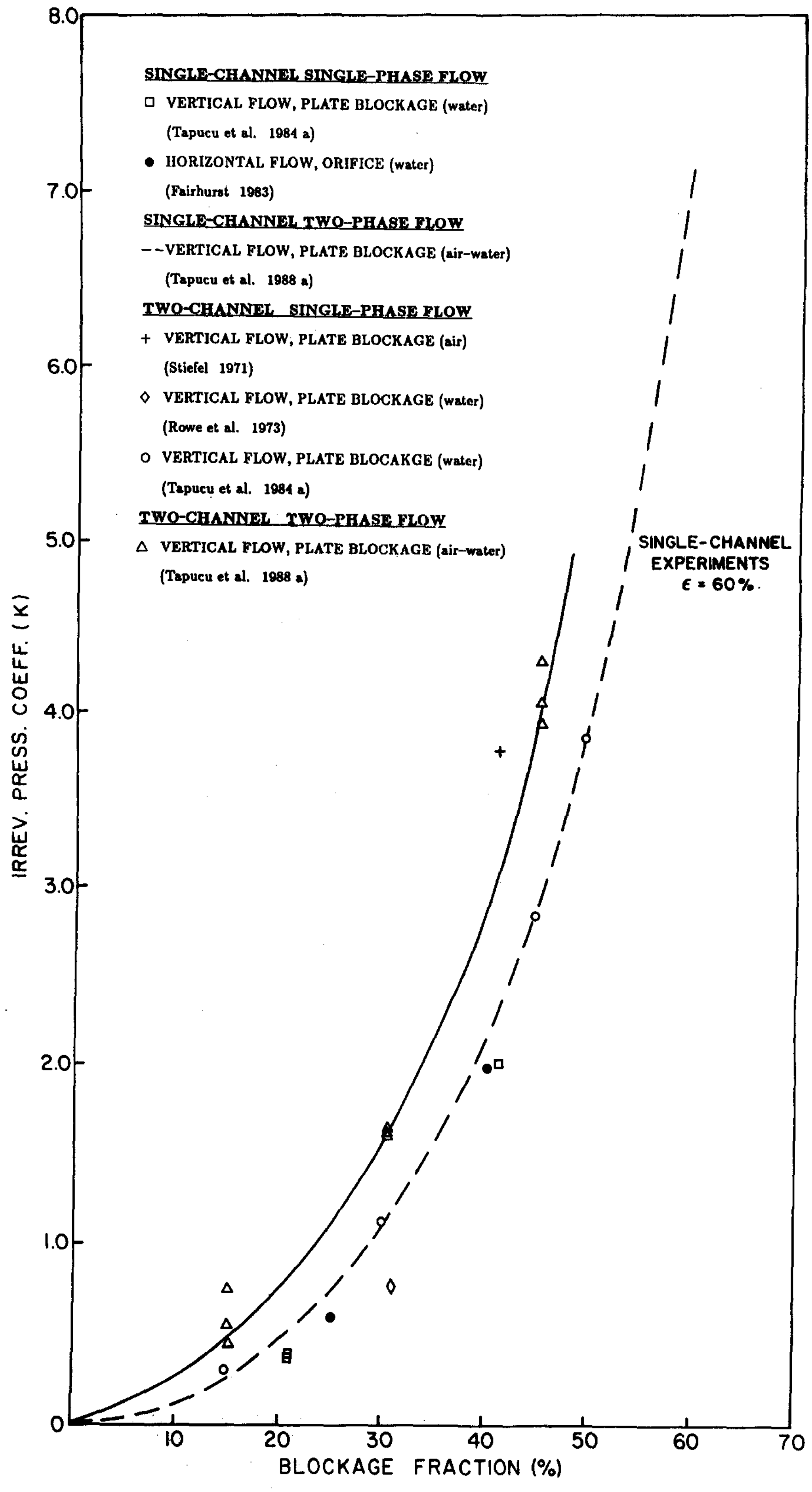


Figure 12. Irreversible form pressure drop coefficient for two-channel flow conditions (plate blockage).

### *Smooth Blockage*

For smooth blockages, the friction and gravity pressure losses between the minimum pressure point upstream of the blockage, and the maximum pressure point downstream of the blockage (points **A** and **B** in figure 5a), are given by

$$\Delta p_{\text{friction}} + \Delta p_{\text{gravity}} = \left(\frac{dp}{dz}\right)_{TP} \Delta z_1 + \int_{-L/2}^{L/2} \Phi_L^2 \left(\frac{dp}{dz}\right)_{f0} dz + \bar{\rho} g L + \left(\frac{dp}{dz}\right)_{TP} \Delta z_2, \quad [8]$$

where $\Delta z_1$ and $\Delta z_2$ are the distances from the minimum and the maximum pressures to the blockage boundaries. The irreversible form pressure drop is then given by

$$\Delta p_{\text{form, TP}} = (p_B - p_A) + \Delta p_{\text{friction}} + \Delta p_{\text{gravity}}. \quad [9]$$

Because of the varying flow section in the blocked area, the integral appearing in [8] is solved numerically by dividing the smooth blockage into 10 equal intervals. The friction factor, $f$, is estimated using (Tapucu *et al.* 1988a)

$$f = 0.0032 + \frac{0.221}{\text{Re}^{0.237}}. \quad [10]$$

Table 4 gives the irreversible form pressure loss coefficients, $K$, and the form two-phase multipliers, $\Phi^2_{\text{form}}$, obtained using [9], [3] and [4]. The two-channel $K$-coefficients are shown in figure 13 along with those obtained under single-channel flow conditions for 60 and 20% void fractions given by Tapucu *et al.* (1988a). As in the case of the plate blockage, the smooth blockage in two interconnected channels produces higher $K$-coefficients than an equivalent blockage in a single channel. This figure also suggests that the pressure loss coefficient increases with increasing void fraction.

## 6. SUMMARY OF THE OBSERVATIONS

### *Axial Pressures Upstream of the Blockage*

(1) In the interconnected region, the pressures in the blocked and unblocked channels are equal and decrease linearly up to the point of onset of diversion cross-flow, caused by the blockage.
(2) After this point, for plate blockages the pressure increases in the blocked channel, whereas for smooth blockages it first increases slightly and then decreases.
(3) For all blockages the pressure in the unblocked channel decreases quite rapidly, due to the acceleration of the flow caused by the lateral inflow.

### *Axial Pressures Downstream of the Blockage*

(4) The pressure in the blocked channel assumes its lowest value just behind the blockage.
(5) The pressure recovery is not complete. The rest dissipates as heat energy, mainly in the recirculation zone; this partial recovery is accomplished over a distance of approx. 60 mm (5 hydraulic diameters).

Table 4. Irreversible form pressure loss coefficient for two-interconnected channels (smooth blockages)

| Run No. | Blockage fraction (%) | Dryness fraction $\bar{x}$ | Void fraction $\bar{\epsilon}$ | $\rho'$ (kg/m$^3$) | Absolute pressure (kPa) | $(\Delta p_{AB})_{TP}$ (Pa) | $\Delta p_f + \Delta p_g$ (Pa) | $\Delta p_{\text{form, TP}}$ (Pa) | $\Delta p_{\text{form, SP}}$ (Pa)[a] | $K_{\text{form, TP}}$ | $\Phi^2_{\text{form}}$ |
|---|---|---|---|---|---|---|---|---|---|---|---|
| 10 | 58.0 | 0.00535 | 0.61 | 389.2 | 155.01 | −10636.6 | −4251.3 | −6385.3 | −150.0 | 1.25 | 42.57 |
| 11 | 58.0 | 0.00256 | 0.49 | 509.6 | 140.27 | −8590.5 | −3873.6 | −4716.9 | −150.0 | 1.22 | 31.45 |
| 12 | 58.0 | 0.00245 | 0.48 | 514.8 | 139.32 | −5876.0 | −2440.4 | −3435.6 | −150.0 | 0.89 | 22.90 |
| 13 | 58.0 | 0.00055 | 0.26 | 736.7 | 129.55 | −4668.0 | −2304.7 | −2363.3 | −150.0 | 0.88 | 15.76 |
| 14 | 88.1 | 0.00550 | 0.61 | 387.1 | 159.05 | −20626.3 | −4880.0 | −15746.4 | NA[b] | 3.05 | — |
| 15 | 88.1 | 0.00252 | 0.49 | 511.5 | 142.65 | −15639.0 | −3555.1 | −12083.8 | NA | 3.10 | — |
| 16 | 88.1 | 0.00246 | 0.49 | 514.7 | 141.31 | −14330.3 | −2798.6 | −11531.6 | NA | 3.01 | — |
| 17 | 88.1 | 0.00058 | 0.27 | 728.2 | 131.97 | −8408.9 | −2550.6 | −5858.3 | NA | 2.15 | — |
| 18 | 88.1 | 0.00029 | 0.16 | 835.7 | 130.22 | −7525.8 | −2432.3 | −5093.5 | NA | 2.14 | — |

[a]Tapucu *et al.* (1984a).
[b]NA = not available.

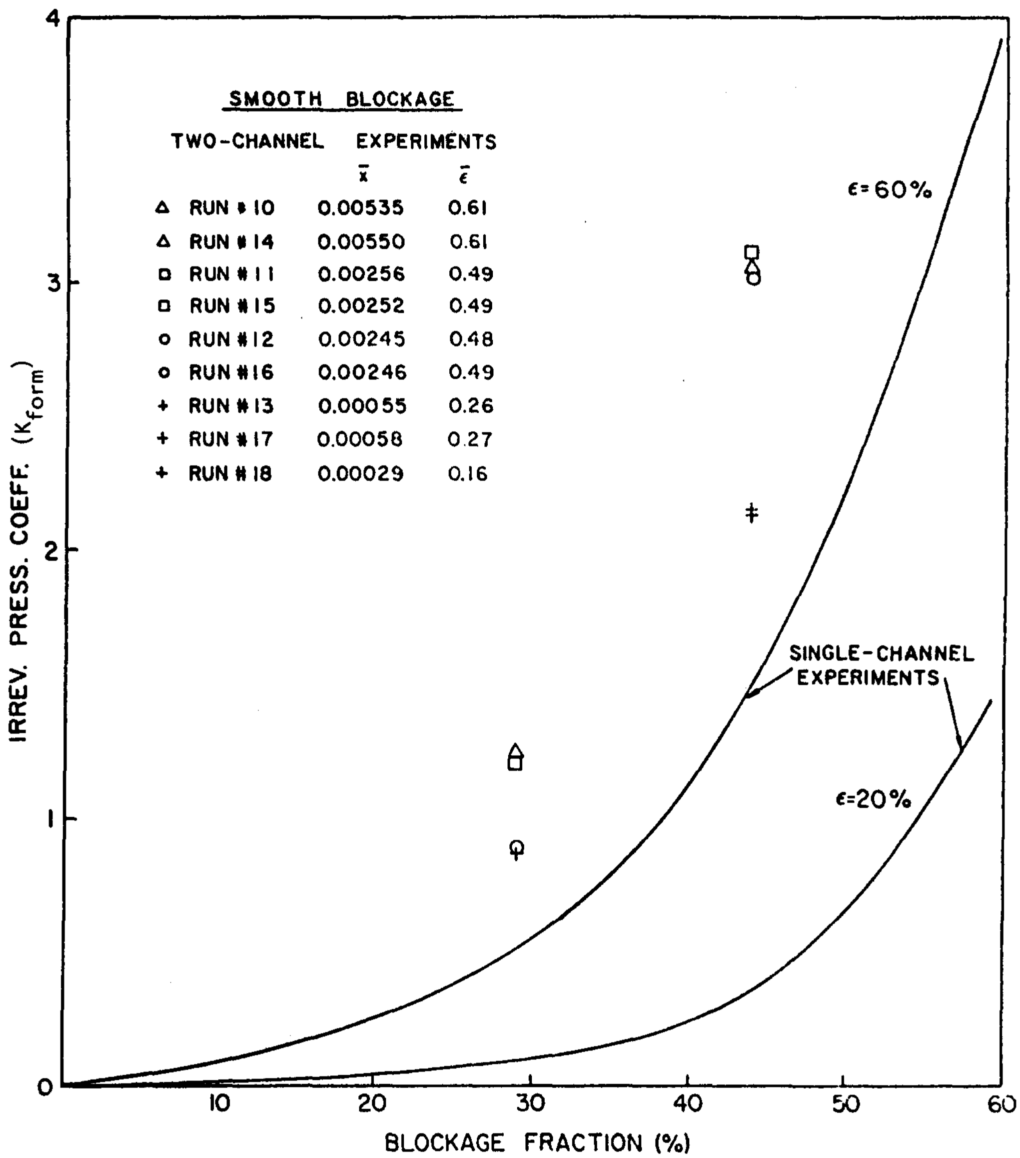


Figure 13. Irreversible form pressure drop coefficient for two-channel flow conditions (smooth blockages).

(6) The pressure drops slowly in the unblocked channel due to the deceleration of the flow and, finally, becomes equal to that in the blocked channel.

(7) The irreversible pressure loss in the interconnected channels depends on the blockage severity and shape, and the void distribution between the channels.

*Pressure Differences Between the Channels Upstream of the Blockage*

(8) The effect of the blockage on the flow is manifested first as a gradual and then as a rapid increase in pressure difference between the channels.

(9) The effect of the blockage on the pressure differences is felt between 100 and 170 mm (8 and 14 hydraulic diameters) upstream of the blockage.

*Pressure Differences Between the Channels Downstream of the Blockage*

(10) In this region, the high pressure prevailing in the unblocked channel drives part of the previously diverted flow back to the blocked channel.

(11) The recovery in the blocked channel of the reversible portion of the static pressure on the one hand, and the kinetic energy of the lateral inflow on the other hand, rapidly reduces the pressure difference between the channels.
(12) The complete equalization of the pressures between the channels requires distances ranging from 80 to 360 mm (7 and 30 hydraulic diameters).

*Acknowledgements*—We are grateful to Messrs R. Desjardins and J. C. Juneau for their technical contributions. This work was funded by the Electric Power Research Institute of California, U.S.A.

## REFERENCES

CHEN, D. K., CHEN, Z. H., ZHAO, Z. S. & ZHUO, N. 1986 The local resistance of gas–liquid two-phase flow through an orifice. *Int. J. Heat Fluid Flow* **7,** 231–238.

FAIRHURST, C. P. 1983 Component pressure loss during two-phase flow. In *Proc. Int. Conf. on the Physical Modelling of Multi-phase Flow*, Coventry, W. Midlands, pp. 1–24.

GENÇAY, S., TAPUCU, A., TROCHE, N. & MERILO, M. 1984 Experimental study of the diversion cross-flow caused by subchannel blockages. Part I—experimental procedures and mass flow rates in the channels. *J. Fluids Engng* **106,** 435–440.

JANSSEN, E. & KERVINEN, J. A. 1964 Two-phase pressure drop across contractions and expansions, water–steam mixtures at 600 to 1400 psia. Report GEAP-4622.

LAFAY, J. & PICUT, M. 1974 Thermo-hydraulique d'un élément de combustion situé au centre d'un canal annulaire localement perturbé par un bouchage partiel. Report CEA–1774.

ROWE, D. W. 1973 A digital computer program for steady state and transient thermal analysis of rod bundle nuclear fuel elements. Report BNWL-1695.

ROWE, D. S., WHEELER, C. L. & FITZSIMMONS, D. E. 1973 An experimental study of flow and pressure in rod bundle subchannels containing blockages. Report BNWL-1771.

SALCUDEAN, M., GROENEVELD, D. C. & LEUNG, L. 1983a Effect of flow obstruction geometry on pressure drops in horizontal air–water flow. *Int. J. Multiphase Flow* **9,** 73–85.

SALCUDEAN, M., CHUN, J. H. & GROENEVELD, D. C. 1983b Effect of flow obstructions on the flow pattern transitions in horizontal two-phase flow. *Int. J. Multiphase Flow* **9,** 87–90.

SALCUDEAN, M., CHUN, J. H. & GROENEVELD, D. C. 1983c Effect of flow obstruction on void distribution in horizontal air–water flow. *Int. J. Multiphase Flow* **9,** 91–96.

SIMPSON, H. C., ROONEY, D. H. & GRATTAN, E. 1979 Two-phase pressure drop in valve and orifice restrictions. Presented at the *Eur. Two-phase Flow Gp Mtg*, Ispra, Italy, Paper E3.

SIMPSON, H. C., ROONEY, D. H. & GRATTAN, E. 1983 Two-phase flow through gate valves and orifice plates. In *Proc. Int. Conf. on the Physical Modelling of Multi-phase Flow*, Coventry, W. Midlands, pp. 25–40.

SPARROW, E. M., RAMSEY, J. W. & LAU, S. C. 1979 Flow and pressure characteristics downstream of a segmental blockage in a turbulent pipe flow. *Trans. ASME* **101,** 200–207.

STIEFEL, U. 1971 Comparison of measured and calculated mass flow distribution in partially blocked parallel flow channels. EIR Report TM-IN-481.

STIEFEL, U. 1972 Berechnung und Messung des Massenquerstromes Zwischen Parallelen Teilkanalen. *Reaktor Tagung, Deutsches Atomforum*, Bonn, Paper 136.

STIEFEL, U. & NOTHIGER, H. 1969 Cross-flow between subchannels. Results of measurements carried out in the MEGAERE-Rig. EIR Report TM-IN-408.

TAPUCU, A. & MERILO, M. 1977a Studies on diversion cross-flow between two parallel flows communicating by a lateral slot. Part I, transverse resistance coefficient. *Nucl. Engng Des.* **42,** 297–306.

TAPUCU, A. & MERILO, M. 1977b Studies on diversion cross-flow between two parallel flows communicating by a lateral slot. Part II, axial pressure variations. *Nucl. Engng Des.* **42,** 307–318.

TAPUCU, A., AHMAD, S. Y. & GENÇAY, S. 1982 Behaviour of two-phase flow in two laterally interconnected subchannels. *Proc. 7th Int. Heat Transfer Conf.* **5,** 361–366.

TAPUCU, A., GENÇAY, S. & TROCHE, N. 1984a Experimental study of the diversion cross-flow caused by subchannel blockages. Vol. I: single-phase flow. EPRI Report NP-3459.

TAPUCU, A., GENÇAY, S., TROCHE, N. & MERILO, M. 1984b Experimental study of the diversion cross flow caused by subchannel blockages. Part II, pressures in the channels and the comparison of the COBRA-III-C predictions with experimental data. *J. Fluids Engng* **106,** 441–447.

TAPUCU, A., TEYSSEDOU, A., GEÇKINLI, N. & TROCHE, N. 1988a Experimental study of the diversion cross-flow caused by subchannel blockages. Vol. II: two-phase flow. EPRI Report NP-3459-2.

TAPUCU, A., GEÇKINLI, M., TROCHE, N. & GIRARD, R. 1988b Experimental investigation of mass exchange between two laterally interconnected two-phase flows. *Nucl. Engng Des.* **105,** 295–312.

TAPUCU, A., TEYSSEDOU, A., TROCHE, N. & MERILO, M. 1989 Pressure losses caused by area changes in a single-channel flow under two-phase flow conditions. *Int. J. Multiphase Flow* **15,** 51–64.

TEYSSEDOU, A., TAPUCU, A., GEÇKINLI, M. & MERILO, M. 1989a Axial void distribution in two laterally interconnected channels with blockages. *Int. J. Multiphase Flow.* **15,** 65–79.

TEYSSEDOU, A., TAPUCU, A., GEÇKINLI, M. & MERILO, M. 1989b Axial mass flow distribution in two laterally interconnected channels with blockages. *Int. J. Multiphase Flow.* **15,** 605–626.

WEISMAN, J., HUSAIN, A. & HARSHE, B. 1978 Two-phase pressure drop across abrupt area changes and restrictions. In *Proceedings of the Two-phase and Heat Transfer Symposium* (Edited by VEZIROGLU, T. N. & KAKAÇ, S.), pp. 1281–1316. Hemisphere, Washington, D.C.